

## Charge-induced spin polarization in nonmagnetic organic molecule Alq<sub>3</sub>

K. Tarafder, B. Sanyal, and P. M. Oppeneer

*Department of Physics and Astronomy, Uppsala University, P.O. Box 516, SE-75120 Uppsala, Sweden*

(Received 15 July 2010; published 31 August 2010)

Electrical injection in organic semiconductors is a key prerequisite for the realization of organic spintronics. Using density-functional theory calculations we report the effect of electron transfer into the organic molecule Alq<sub>3</sub>. Our first-principles simulations show that electron injection spontaneously spin-polarizes nonmagnetic Alq<sub>3</sub> with a magnetic moment linearly increasing with induced charge. An asymmetry of the Al-N bond lengths leads to an asymmetric distribution of injected charge over the molecule. The spin polarization arises from a filling of dominantly the nitrogen  $p_z$  orbitals in the molecule's lowest unoccupied molecular orbital together with ferromagnetic coupling of the spins on the quinoline rings.

DOI: 10.1103/PhysRevB.82.060413

PACS number(s): 87.15.-v, 85.75.-d, 71.15.Mb

Organic semiconductors (OSCs) are contemporary being considered as prospective materials for spintronics applications.<sup>1,2</sup> As OSCs primarily consist of  $\pi$ -conjugated molecules composed of atoms with low atomic numbers, the spin-orbit and nuclear hyperfine interactions are weak. OSCs therefore exhibit typically very long spin-relaxation times,<sup>3</sup> a property favorable for spin transport. Moreover, owing to the availability of a large variety of OSCs and the possibility to chemically tailor specific functionalities, there is a huge potential for the development of versatile, low-cost organic spintronic devices.<sup>4,5</sup>

A key prerequisite for the realization of organic spintronics is the realization of electrical injection in the organic layer. Recently, the injection of spin-polarized carriers from a ferromagnetic contact into an OSC has been demonstrated.<sup>6,7</sup> Notwithstanding this affirmative observation, not all OSC materials are comparably well suited for organic spintronics. In particular, the  $\pi$ -conjugated OSC tris(8-hydroxyquinoline) aluminum (Alq<sub>3</sub>) has been discovered to perform very good in organic spin valves, providing one of the best giant magnetoresistance (GMR) values.<sup>1</sup> Alq<sub>3</sub> is a relatively well-known material that is widely used as component in organic light-emitting diodes.<sup>8,9</sup> However, in spite of this, it is not understood why precisely Alq<sub>3</sub> gives rise to extremely long spin-relaxation times,<sup>3</sup> to a high GMR,<sup>1,10</sup> and significant tunnel magnetoresistance values.<sup>11</sup>

Here we employ density-functional theory (DFT) calculations to explore the influence of electron injection into Alq<sub>3</sub>. Our first-principles calculations reveal that electron charging causes, unexpectedly, a spin polarization of the organic molecule, which is nonmagnetic in its neutral state. The origin of the appearing spin polarization is analyzed in detail and shown to be connected to the small asymmetry of the  $\pi$ -conjugated rings, i.e., a feature that is closely related to the particular molecular geometry and molecular orbitals of Alq<sub>3</sub>. The here-reported influence of electron injection in Alq<sub>3</sub> provides an essential ingredient to a microscopic understanding of the complex spin-polarized transport in Alq<sub>3</sub>.

Since Alq<sub>3</sub> is widely used as a material in organic electroluminescent devices,<sup>8,9</sup> a number of experimental as well as theoretical studies have been performed for this material. Using DFT calculations, photoemission, and near edge x-ray absorption fine structure, Andreoni and co-workers<sup>12</sup> have characterized the structural and electronic properties of Alq<sub>3</sub>

in both neutral and charged states, which provided a picture of the orbital structure of Alq<sub>3</sub>. Johansson *et al.*<sup>13</sup> used a combination of x-ray and ultraviolet photoemission spectroscopy with DFT calculations to discuss the interaction of Alq<sub>3</sub> with Li and K. Recently, the geometrical and electronic structures of Alq<sub>3</sub> interacting with Mg and Al have also been investigated using DFT calculations.<sup>14,15</sup> Baik *et al.*<sup>16</sup> tried to make this material magnetic by Co doping. Zhan *et al.*<sup>17</sup> studied the interaction of Alq<sub>3</sub> with an Fe surface. Using DFT, semiempirical, and *ab initio* molecular-orbital theories, Zhang *et al.*<sup>18</sup> studied the effect of electrical charging on the electronic structure of Alq<sub>3</sub>. However, these studies have not considered any geometric structural change in the molecule due to charge injection, nor any magnetic effects.

We have performed first-principles DFT calculations using the full-potential Vienna *ab initio* simulation package (VASP) (Ref. 19) which uses pseudopotentials and the projector augmented wave approach. We used the Perdew-Burke-Ernzerhof generalized gradient approximation (GGA) for treating the exchange-correlation potential. A sufficiently high-energy cutoff (550 eV) was used in each calculation to obtain accurate results. In our simulations the forces on each of the atoms were calculated using the Hellmann-Feynman theorem, and were subsequently used to perform a conjugate gradient structural relaxation. The structural optimizations were continued until the forces on the atoms converged to less than 1 meV/Å. This optimization has been completely carried through for each Alq<sub>3</sub> molecule with an additional charge. There are two isomers of Alq<sub>3</sub>, namely, *facial* and *meridional* with C<sub>3</sub> and C<sub>1</sub> point-group symmetries, respectively. Of these two, the meridional isomer is reported<sup>12,20</sup> to possess the lowest formation energy. This we have also confirmed in our calculations. In the following we consider therefore only meridional Alq<sub>3</sub>.

The molecular structure of the meridional isomer is shown in Fig. 1. The Al atom is surrounded by three nearly planar nitrogen atoms as well as by three nearly planar oxygen atoms, being the link to the quinolines that consists of a pyridine and a benzene ring. In our study we first adopted the experimental structure (see, e.g., Ref. 20) and performed a full geometric relaxation for the neutral ground state. Subsequently, we used this DFT-computed ground-state geometry and added extra charges (indicated later on by  $q$ ) on the molecule to simulate the charge injection and repeated the

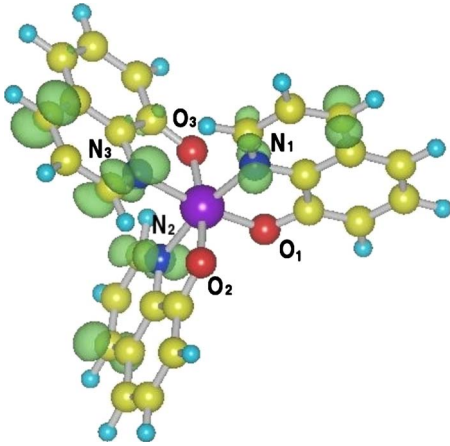


FIG. 1. (Color online) Geometry and charge-induced magnetization density of meridional  $\text{Alq}_3$ . Al, O, N, C, and H atoms are shown as (large) magenta, (dark gray) red, (gray) blue, (light gray) yellow, and (small) turquoise spheres, respectively. The magnetization density of the charged  $\text{Alq}_3$  molecule with one extra electron is shown by the green (gray) hyper surface.

full atomic relaxation procedure, assuming an equivalent neutralizing background in the simulation cell. Note that the added charge is not set to have any fixed spin. Since in the charged molecule there will always be a net electric-dipole moment, the dipole correction has also been included in our calculation. We have also tried positive charging, i.e., extracting electron charge from the molecule. However, we find that in this case the molecule become very unstable and we are not able to converge to a stable molecular geometry. This finding is, in fact, consistent with an experimental investigation that shows a very high positive charge injection energy as compared to a low energy for negative-charge injection.<sup>21</sup>

To start with, we compare our geometry optimized ground-state structure of  $\text{Alq}_3$  with available theoretical and experimental data, which are summarized in Table I. Previous studies showed that structural parameters of meridional  $\text{Alq}_3$  in good agreement with experiment could be obtained using Hartree-Fock (HF) calculations with the  $3-21+G^{**}$  basis set.<sup>20</sup> A somewhat less good agreement was achieved with hybrid-functional B3LYP calculations<sup>13,22</sup> [using the

TABLE I. Ground-state Al-N and Al-O bond lengths (in Å), for neutral meridional  $\text{Alq}_3$  from different theoretical calculations (Refs. 13, 20, and 22), including this work, and experimental results (Ref. 20) (averaged over several available data sets).

Bond	HF, 3-21+ $G^{**}$ (Ref. 20)	B3LYP, 6-31G(d) (Ref. 22)	B3LYP, DNP (Ref. 13)	Exp. ave. (Ref. 20)	GGA our calc.
Al-N <sub>1</sub>	2.063	2.08	2.019	2.044	2.063
Al-N <sub>2</sub>	2.033	2.06	2.019	2.025	2.050
Al-N <sub>3</sub>	2.117	2.13	2.051	2.079	2.103
Al-O <sub>1</sub>	1.826	1.86	1.839	1.847	1.865
Al-O <sub>2</sub>	1.866	1.89	1.868	1.867	1.888
Al-O <sub>3</sub>	1.856	1.88	1.864	1.856	1.886

TABLE II. Ground state Al-N and Al-O bond lengths for meridional  $\text{Alq}_3$  upon injection with 0.5 and 1.0 electron, respectively.

Bond	0.5e (in Å)	1.0e (in Å)
Al-N <sub>1</sub>	2.076	2.073
Al-N <sub>2</sub>	2.042	2.031
Al-N <sub>3</sub>	2.065	2.048
Al-O <sub>1</sub>	1.877	1.887
Al-O <sub>2</sub>	1.899	1.905
Al-O <sub>3</sub>	1.889	1.896

6-31G(d) basis set and the double numerical plus polarization (DNP) basis]. It can be observed from Table I that our GGA calculations yield structural results which are in very good agreement with previous Hartree-Fock<sup>20</sup> and recent B3LYP calculations.<sup>22</sup>

One observes from the structural data that the Al is bonded more closely to the oxygen atoms than the nitrogen atoms, and that it has different bond lengths to the six ligands. The N<sub>3</sub> atom has the largest separation from Al whereas N<sub>1</sub> and N<sub>2</sub> have similar bond lengths with Al. The three Al-O bond lengths are more equal. Given the different Al-N bond lengths in an otherwise symmetric arrangement, an influence of charge doping on the molecule is not surprising. It is therefore interesting to examine the behavior of the molecule upon electron charging.

Table II shows the structural change in the molecule due to electron charging. Compared to the charge-neutral structure, the Al-N<sub>2</sub>, Al-N<sub>3</sub> bond lengths are reduced, Al-N<sub>1</sub> becomes slightly longer. The Al-O<sub>1</sub> bond length also becomes longer but the Al-O<sub>2</sub> and Al-O<sub>3</sub> distances are not changed as much. The change is gradual with the amount of charging of the molecule. The influence of the charge is most prominent for the N<sub>3</sub> atom having initially the maximum bond length. We further observe that the asymmetry of the three Al-O bond lengths is reduced with charging.

Our calculations reveal that upon electron charging the nonmagnetic  $\text{Alq}_3$  molecule spontaneously spin polarizes. Figure 2 shows the development of the molecule's spin moment due to the added charge. The magnetic moment of the

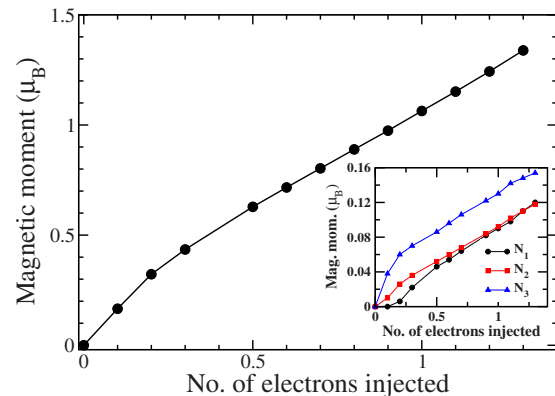


FIG. 2. (Color online) Magnetic spin moment of  $\text{Alq}_3$  as a function of injected electron charge. In the inset, the projected moments on the three N atoms are shown with the added electron charge.

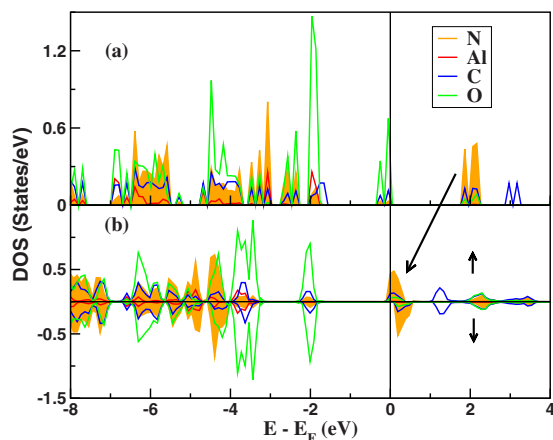


FIG. 3. (Color online) Atom projected DOS of the  $\text{Alq}_3$  molecule shown in (a) for the nonmagnetic, charge neutral, and in (b) for the molecule with 1.0 electron doping. In (b), the spin-resolved partial DOS is shown. The arrow indicates the shift of the LUMO to the Fermi energy ( $E_F$ ). Note that the N states of the LUMO become spin polarized upon charging.

molecule increases approximately linearly with the extra charge. This is a surprising result because the extra charge could be equally distributed over the two spin channels of a molecular orbital, leading to a nonmagnetic charged molecule but this does not happen. A key to understanding why this is the case is the asymmetric bonding in the neutral molecule. The added electron charge does not distribute equally over the three nitrogen atoms but it goes dominantly to the  $\text{N}_3$  atom. In Fig. 1 the magnetization density corresponding to  $q=1.0e$  is shown by the hypersurface. It is clearly observed that the magnetization density resides prominently on the three N atoms. For this relatively high  $q$  value, the carbon atoms of the pyridine ring display also some magnetization density, corresponding to magnetic moments of  $0.08 \mu_B$  on the average. This magnetization density resides mainly on one of the carbon atoms nearest to nitrogen, as well as on the third-nearest-neighbor carbon atom. Neither O nor Al atoms carry a magnetic moment.

From the above we deduce that the magnetic moment arising due to electron charging is related mostly to the N atoms. To understand this further, we have plotted the local magnetic moments on the three nitrogen atoms as a function of extra electron charge on the molecule. This is shown in the inset of Fig. 2. The magnetic moments on the  $\text{N}_1$  and  $\text{N}_2$  atoms are varying in a similar manner whereas the curve for  $\text{N}_3$  is separated from that of  $\text{N}_1$  and  $\text{N}_2$ . Over the full range of charging, the  $\text{N}_3$  atom has acquired a larger magnetic moment than the other two N atoms. This behavior corroborates with the structural change upon charging. As discussed earlier, the decrease in the Al- $\text{N}_3$  bond length is more significant than that of Al- $\text{N}_1$  and Al- $\text{N}_2$ . This larger bond-length reduction appears to be related to the steeper increase in the magnetic moment of  $\text{N}_3$ . The Al-O bond lengths are not modified appreciably with extra charge and consistently no spin polarization on the oxygen atoms is observed.

The atom-projected density of states (DOS) are shown in Fig. 3 for both neutral and a molecule charged with  $q=1.0e$ . The highest Al  $p$  states occur at 2 eV binding en-

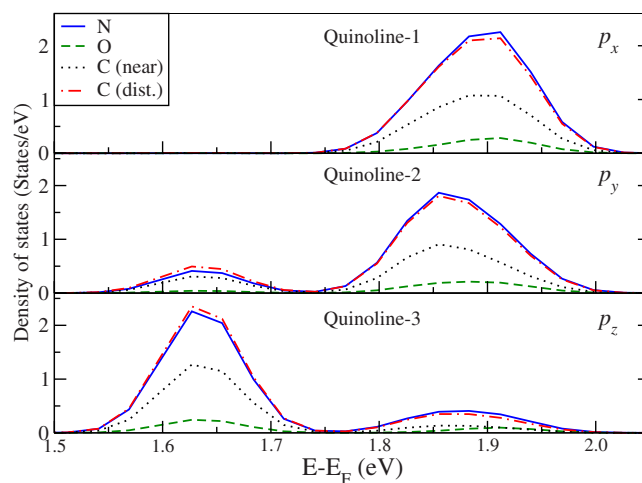


FIG. 4. (Color online) Atom-resolved  $p$  partial DOS of the lowest unoccupied molecular orbitals of  $\text{Alq}_3$ , shown separately for the three quinoline groups (labeled in Fig. 1). The  $p$  states of the quinoline-3 farthest away from Al have the lowest energy.

ergy. The Al orbitals are hence saturated with covalent bonds to the oxygen atoms and nitrogen atoms. The Al  $3p$  shell is in fact over saturated in the sixfold coordination, which explains why one nitrogen, here  $\text{N}_3$ , has a longer distance to Al. The quinoline ring is, however, structurally very stable, giving not much spatial freedom for a longer Al-N distance. As can be seen from Fig. 3(a) for the neutral molecule, the highest occupied molecular orbital (HOMO) level has mainly O  $p$  character whereas the lowest unoccupied molecular orbital (LUMO) consists of mainly N  $p$  states with a small admixture of O and C states. Al has a negligible contribution to both HOMO and LUMO. The calculated HOMO-LUMO gap is 1.87 eV. Upon charging, the N  $p$  states in the LUMO become spin polarized and the HOMO-LUMO gaps for the spin-up and spin-down channels increase to 2.0 eV and 2.2 eV, respectively. The HOMO states remain practically nonpolarized.

The origin of the unexpected magnetization in the electron-injected state can be understood from the following observations. Due to the molecule's asymmetry the unoccupied N  $p$ -dominated states at 1.8 eV occur at slightly different energies, with the  $\text{N}_3$  related states occurring at a somewhat lower energy. Figure 4 shows the unoccupied  $p$  partial DOS of the atoms in the three quinoline rings. Note that we have broadened the DOS peaks, leading to a shift to lower energies. The LUMO consists only of atomic  $p$ -type orbitals, no other type is present. One can observe that electron doping commences with initially filling the empty  $p_z$  levels of  $\text{N}_3$ . Hence, the moment on  $\text{N}_3$  increases at first steeply with doping. Due to the small asymmetry and the structural relaxation, the empty  $p_x$  and  $p_y$  states of  $\text{N}_1$  and  $\text{N}_2$  start to be filled more slowly. Note that these are equivalent to the  $\text{N}_3$   $p_z$  orbitals by rotation. Electron doping of more than  $0.5e$  leads to an increase in the moments on all three nitrogen atoms at the same rate. For the narrow  $p_z$  orbitals spin-polarized filling is more favorable than equal filling of both spin orbitals (Pauli principle). A somewhat larger electron filling would lead to an equal filling of both spin orbitals on one nitrogen

and thus to a nonmagnetic state but this does not happen because the unoccupied  $p_z$  orbitals of the other two nitrogen atoms are preferably being filled first, which causes a small moment on  $N_1$  and  $N_2$  as well. A ferromagnetic coupling between the three spin moments stabilizes finally a net spin polarization on the whole molecule.

To conclude, our DFT calculations reveal that electron injection in  $Alq_3$  leads to spontaneous spin polarization. The predicted spin polarization reaches to  $1 \mu_B$  per injected electron per molecule. The spin polarization is found to originate from the preferential spin-polarized filling of empty N  $p_z$  orbitals in the LUMO, in combination with a parallel coupling

between the spins on the quinolines. This discovered induced spin polarization of the normally nonmagnetic  $Alq_3$  molecule can be expected to be critically related to the extremely long spin-relaxation times observed in  $Alq_3$  (Ref. 3) as well as to be essential for the observed large magnetoresistance.<sup>1,23</sup>

We thank Y. Zhan and O. Eriksson and helpful discussions. This work has been supported financially by the Swedish Research Council (VR), SIDA, the C. Tryggers Foundation, and STINT. Computational support from the Swedish National Infrastructure for Computing (SNIC) is also acknowledged.

- 
- <sup>1</sup>Z. H. Xiong, D. Wu, Z. V. Vardeny, and J. Shi, *Nature (London)* **427**, 821 (2004).
- <sup>2</sup>W. J. M. Naber, S. Faez, and W. G. van der Wiel, *J. Phys. D* **40**, R205 (2007).
- <sup>3</sup>S. Pramanik, C.-G. Stefania, S. Patibandla, S. Bandyopadhyay, K. Garre, N. Harth, and M. Cahay, *Nat. Nanotechnol.* **2**, 216 (2007).
- <sup>4</sup>V. A. Dediu, L. E. Hueso, I. Bergenti, and C. Taliani, *Nature Mater.* **8**, 707 (2009).
- <sup>5</sup>F. Pulizzi, *Nature Mater.* **8**, 691 (2009).
- <sup>6</sup>M. Cinchetti, K. Heimer, J.-P. Wüstenberg, O. Andreyev, M. Bauer, S. Lach, C. Ziegler, Y. Gao, and M. Aeschlimann, *Nature Mater.* **8**, 115 (2009).
- <sup>7</sup>A. J. Drew *et al.*, *Nature Mater.* **8**, 109 (2009).
- <sup>8</sup>C. W. Tang and S. A. VanSlyke, *Appl. Phys. Lett.* **51**, 913 (1987).
- <sup>9</sup>S. A. Van Slyke, C. H. Chen, and C. W. Tang, *Appl. Phys. Lett.* **69**, 2160 (1996).
- <sup>10</sup>We note that in some spin-valve structures a smaller GMR value was obtained, see, e.g., J. S. Jiang, J. E. Pearson, and S. D. Bader, *Phys. Rev. B* **77**, 035303 (2008).
- <sup>11</sup>T. S. Santos, J. S. Lee, P. Migdal, I. C. Lekshmi, B. Satpati, and J. S. Moodera, *Phys. Rev. Lett.* **98**, 016601 (2007).
- <sup>12</sup>A. Curioni, M. Boero, and W. Andreoni, *Chem. Phys. Lett.* **294**, 263 (1998).
- <sup>13</sup>N. Johansson, T. Osada, S. Stafström, W. R. Salaneck, V. Parente, D. A. dos Santos, X. Crispin, and L. J. Bredas, *J. Chem. Phys.* **111**, 2157 (1999).
- <sup>14</sup>S. Meloni, A. Palma, J. Schwartz, A. Kahn, and R. Car, *J. Am. Chem. Soc.* **125**, 7808 (2003).
- <sup>15</sup>R. Q. Zhang, W. C. Lu, C. S. Lee, L. S. Hung, and S. T. Lee, *J. Chem. Phys.* **116**, 8827 (2002).
- <sup>16</sup>J. M. Baik, Y. Shon, S. J. Lee, Y. H. Jeong, T. W. Kang, and J.-L. Lee, *J. Am. Chem. Soc.* **130**, 13522 (2008).
- <sup>17</sup>Y. Zhan, E. Holmström, R. Lizárraga, O. Eriksson, X. Liu, F. Li, E. Carlegrim, S. Stafström, and M. Fahlman, *Adv. Mater.* **22**, 1626 (2010).
- <sup>18</sup>R. Q. Zhang, C. S. Lee, and S. T. Lee, *Chem. Phys. Lett.* **326**, 413 (2000).
- <sup>19</sup>G. Kresse and J. Hafner, *Phys. Rev. B* **47**, 558 (1993); G. Kresse and J. Furthmüller, *ibid.* **54**, 11169 (1996).
- <sup>20</sup>M. D. Halls and H. B. Schlegel, *Chem. Mater.* **13**, 2632 (2001).
- <sup>21</sup>T. Anazawa, M. Tsukada, and Y. Kataoka, *Microelectron. Eng.* **81**, 222 (2005).
- <sup>22</sup>R. L. Martin, J. D. Kress, I. H. Campbell, and D. L. Smith, *Phys. Rev. B* **61**, 15804 (2000).
- <sup>23</sup>C. Barraud, P. Seneor, R. Mattana, S. Fusil, K. Bouzehouane, C. Deranlot, P. Graziosi, L. Hueso, I. Bergenti, V. Dediu, F. Petroff, and A. Fert, *Nat. Phys.* **6**, 615 (2010).